ACS SyntheticBiology

pubs.acs.org/synthbio Research Article

Metabolic Engineering for Efficient Ketocarotenoid Accumulation in the Green Microalga *Chlamydomonas reinhardtii*

Sofia Amendola, Jacob S. Kneip, Florian Meyer, Federico Perozeni, Stefano Cazzaniga, Kyle J. Lauersen, Matteo Ballottari, and Thomas Baier*

Cite This: *ACS Synth. Biol.* 2023, 12, 820–831 Read Online

ACCESS | Metrics & More | Article Recommendations

ABSTRACT: Astaxanthin is a valuable ketocarotenoid with various pharmaceutical and nutraceutical applications. Green microalgae harbor natural capacities for pigment accumulation due to their 2-*C*-methyl-D-erythritol 4-phosphate (MEP) pathway. Recently, a redesigned ß-carotene ketolase (BKT) was found to enable ketocarotenoid accumulation in the model microalga *Chlamydomonas reinhardtii*, and transformants exhibited reduced photoinhibition under high-light. Here, a systematic screening by synthetic transgene design of carotenoid pathway enzymes and overexpression from the nuclear genome identified phytoene synthase (PSY/crtB) as a bottleneck for carotenoid accumulation in *C. reinhardtii*. Increased ß-carotene hydroxylase (CHYB) activity was found to be essential for engineered astaxanthin accumulation. A combined BKT, crtB, and CHYB expression strategy resulted in a volumetric astaxanthin production of 9.5 ± 0.3 mg L^{-1} (4.5 ± 0.1 mg g^{-1} CDW) in mixotrophic and 23.5 mg L^{-1} (1.09 mg L^{-1} h^{-1}) in high cell density conditions, a 4-fold increase compared to previous reports in *C. reinhardtii*. This work presents a systematic investigation of bottlenecks in astaxanthin accumulation in *C. reinhardtii* and the phototrophic green cell factory design for competitive use in industrial biotechnology.

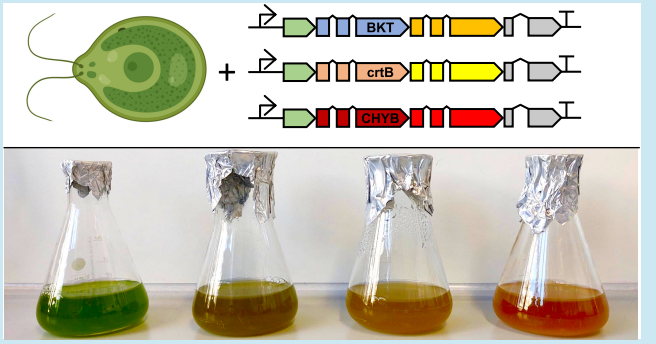

KEYWORDS: *astaxanthin, Chlamydomonas reinhardtii, engineered ketocarotenoid production, metabolic engineering, β-carotene ketolase, β-carotene hydroxylase, phytoene synthase*

INTRODUCTION

High-value ketcarotenoidastaxanthin is one of the most important pigments in biotechnology and is assumed to have various health benefits after human consumption.[1] It contains two terminal *β*-ionone-type residues and an extended carbon chain with conjugated double bonds, which confer high antioxidant properties and its characteristic orange-red color. Astaxanthin-containing feed yields red pigmentation in farmed fish and shellfish (e.g., salmon, trout shrimps, and crayfish) and promotes higher customer acceptance and market value (US $550 million globally in 2017).[2] Natural astaxanthin accumulation is present in only a few microorganisms, including selected microalgae (*Haematococcus lacustris*, *Chlamydomonas nivalis*, *Chromochloris zofingiensis*, *Euglena sanguinea*, *Scenedesmus* ssp., *Nannochloropsis* spp.), carotenogenic bacteria (e.g., *Paracoccus* spp., *Sphingomonas* spp., and *Brevundimonas* spp.), selected fungi (e.g., *Xanthophyllomyces dendrorhous*), and few plant flowers (e.g., *Adonis* ssp.)[3−5] However, slow growth rates and inefficient extraction, as observed in *H. lacustris* aplanospores, reduce (bio-)accessibility from native sources and raise demand for efficient alternatives.[1,6]

Carotenoid biosynthesis starts from glyceraldehyde 3-phosphate (G3P) and pyruvate, which are used to create C_5 isopentenyl pyrophosphate (IPP) and dimethylallyl pyrophosphate (DMAPP) through the 2-*C*-methyl-D-erythritol 4-phosphate (MEP) pathway in plastids and bacteria. These C_5 building blocks are condensed to the intermediate C_{20} geranylgeranyl pyrophosphate (GGPP) and subsequently to the colorless C_{40} carotenoid phytoene. After desaturation to lycopene, the pathway branches into *α*- and ß-carotenes. The ß-carotene path enables the synthesis of the xanthophylls, zeaxanthin and violaxanthin, which are bound by antenna proteins of photosystems, increase light harvesting efficiency, serve as major energy quenching molecules, and play important roles in cellular protection against excessive light and reactive oxygen species (ROS).[7] The final synthesis of

Received: November 15, 2022
Published: February 23, 2023

https://doi.org/10.1021/acssynbio.2c00616
ACS Synth. Biol. 2023, 12, 820−831

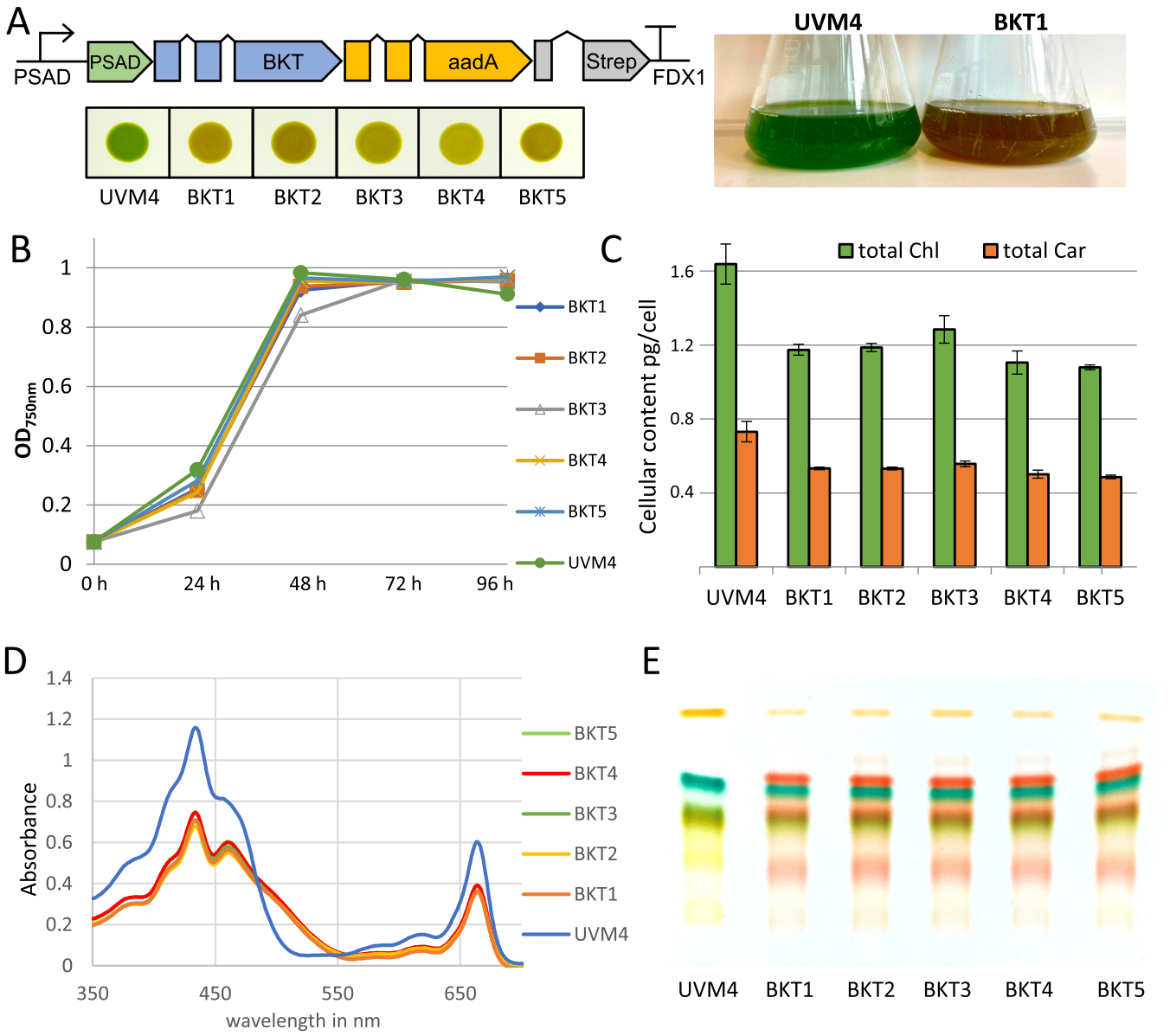

Figure 1. Establishment of non-native ketocarotenoid accumulation and characterization of derived transformants. (A) *C. reinhardtii* UVM4 and transformants derived from the integration of a synthetically optimized *Cr*BKT construct. BKT expression was designed as protein fusion to an antibiotic resistance marker (aminoglycoside adenylyltransferase, aadA) including a PSAD CTP and C-terminal StrepII-tag. Transcription was driven by PSAD promoter and FDX1 terminator. Transformants exhibit a characteristic brown coloration. (B) Optical density recorded for *C. reinhardtii* UVM4 and five randomly isolated transformants. Cultivation was performed in 100 mL Erlenmeyer flasks under mixotrophic conditions with 350 μmol photons m^{-2} s^{-1}. Results represent mean values and standard deviation from biological triplicates (n = 3). (C) Cellular chlorophyll and carotenoid contents were quantified in acetone extracts after 72 h of mixotrophic cultivation. Results represent mean values and standard deviation from biological triplicates (n = 3). (D) Photometric measurement of acetone extracts from *C. reinhardtii* UVM4 and BKT-expressing transformants. (E) Thin-layer chromatography of acetone extracts from *C. reinhardtii* UVM4 and BKT-expressing transformants.

astaxanthin is achieved by oxidation of both zeaxanthin β-rings or alternatively of β-carotene into canthaxanthin, followed by hydroxylation.[8,9] Heterologous astaxanthin biosynthesis has been established in several heterotrophic microbes including *Escherichia coli*,[10,11] *Corynebacterium glutamicum*,[12,13] and *Saccharomyces cerevisiae*.[14,15] Heterologous production in microbial hosts typically involves carotenoid pathway reconstitutions using both, pro- and eukaryotic pathway enzymes as well as enhancing flux toward isoprenoid biosynthesis by modification of MEP/mevalonate (MVA) pathways. Fermentative hosts can achieve relatively high volumetric production titers of heterologous astaxanthin. In engineered *E. coli*, up to 1.18 g L^{-1} astaxanthin (7.8 mg g^{-1} CDW) after 60 h of fed-batch fermentation has been reported.[11] The promiscuous nature of enzymes involved in astaxanthin biosynthesis leads to the accumulation of several intermediates and side products in conjunction with the target product, which can lower bioprocess efficiencies.[16]

A key enzyme in the biosynthesis of astaxanthin is the ß-carotene ketolase (BKT), which catalyzes the conversion of zeaxanthin to astaxanthin and ß-carotene to canthaxanthin at high efficiency.[17−19] Several isoforms of this enzyme exist and recently, *Chlamydomonas reinhardtii* BKT (*Cr*BKT) has been characterized through its heterologous overexpression in

https://doi.org/10.1021/acssynbio.2c00616
ACS Synth. Biol. 2023, 12, 820−831

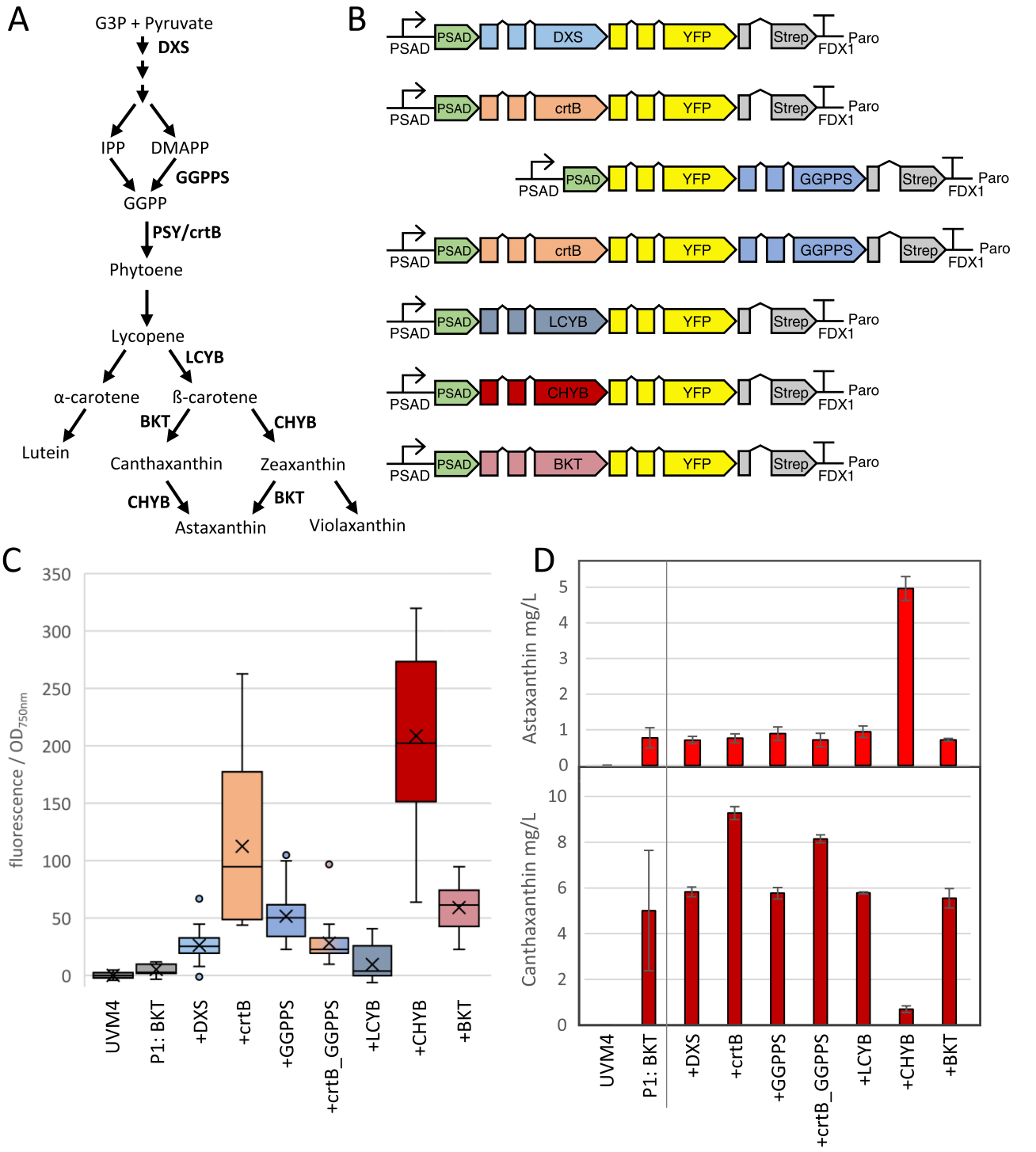

Figure 2. Metabolic engineering of a CrBKT-expression transformant including the coexpression of enzymes involved in the MEP and carotenoid biosynthesis pathway. (A) Schematic of the 2-*C*-methyl-D-erythritol 4-phosphate/1-deoxy-D-xylulose 5-phosphate (MEP) and carotenoid biosynthesis pathway present in *C. reinhardtii*. Enzymes are depicted, which were identified as potential bottlenecks toward astaxanthin biosynthesis. (B) Genetic constructs designed for coexpression in the CrBKT background strain (BKT1, Figure 1). Coding sequences were synthetically optimized as previously described[25,27] and designed as fusion proteins to a yellow fluorescence reporter (mVenus, YFP), with a PSAD-targeting peptide[78] and C-terminal StrepII-tag. Transcription was driven by the PSAD promoter[78] and the FXD1 terminator.[84] All plasmids used for the second iteration of nuclear transformation contain an APHVIII paromomycin resistance cassette for selection (Paro).[85] (C) Box and whisker plot representing the measured fluorescence intensity of the 20 best-expressing transformants from 288 randomly isolated colonies. Transformants were individually cultivated in 24-well microtiter plates, and fluorescence was quantified using a microtiter plate reader with respective filter settings. The minimum (lowest line), lower quartile (bottom of the box), median (central line), mean (cross), upper quartile (top of the box), maximum (top line), and outliers (dots) are depicted. (D) Pigment quantification of pooled samples from the best 20 expressing transformants after individual transformant cultivation for 72 h in microtiter plates under mixotrophic conditions. Quantification was performed in technical triplicates by HPLC, and the results represent mean values and standard deviation (n = 3).

https://doi.org/10.1021/acssynbio.2c00616
ACS Synth. Biol. 2023, 12, 820−831

several photosynthetic host organisms including *Physcomitrium patens*,[20] *Solanum lycopersicum*,[21,22] *Oryza sativa*,[23,24] and *Arabidopsis thaliana*.[17] Natively, *Cr*BKT expression is exclusively limited to the zygospore state in *C. reinhardtii* and is completely silenced in the green haploid vegetative state.[16,19] Recently, *Cr*BKT was overexpressed in vegetative *C. reinhardtii* cells by synthetic redesign for high transgene expression[25−27] and removal of a 116 amino acid long, low-complexity region from the C-terminus.[19] Under optimal growth conditions, a *Cr*BKT overexpressing *C. reinhardtii* transformant was found to accumulate up to ∼6 mg L^{-1} (2.5 mg g^{-1} CDW) ketocarotenoids,[19,28] and transformants exhibited reduced photoinhibition under high light.[28] *Cr*BKT overexpression led to a clear modification of the pigment profile and co-accumulation of astaxanthin and larger amounts of other ketocarotenoid intermediates, including canthaxanthin. The accumulation of several partially ketolated intermediate carotenoids in addition to astaxanthin may have been due to the lower activity of other enzymes responsible for further functionalization, which are not natively expressed at levels that balance the engineered overexpression of the *Cr*BKT. To date, no further metabolic optimization to enhance astaxanthin accumulation in this algal host has been reported.

Metabolic engineering in the model green microalga *C. reinhardtii* has recently become attainable through advances in strain domestication and transgene design, which has led to many recent reports demonstrating the potential of this alga as a green cell factory for the bioproduction of many valuable compounds.[27,29−36] In combination with genomically optimized strains and the culture medium designed to yield high-cell-density photoautotrophic production, the cultivation of *C. reinhardtii* at industrially viable scales is now within reach.[32,37] As a photosynthetic organism, *C. reinhardtii* has naturally a high flux of fixed carbon toward pigment turnover to cope with fluctuating light conditions, contains a complex carotenoid biogenesis pathway (including a native ß-carotene hydroxylase), is generally regarded as safe (GRAS),[38] and astaxanthin from the algal biomass has been shown to have a high bioavailability.[19] Recently, *C. reinhardtii* has been successfully engineered to produce substantial levels of heterologous terpenoids at considerable carbon partitioning levels without growth interference.[33,39,40] These features set *C. reinhardtii* apart as a promising chassis for scalable bioproduction of astaxanthin.

In this study, we demonstrate the first systematic metabolic engineering of *C. reinhardtii* to enhance the flux from precursors into the desired ketocarotenoid astaxanthin. We employed a combination of native and foreign gene redesign for their overexpression from the algal nuclear genome. Our efforts allowed the systematic investigation of carotenoid pathway limitations, to channel intermediates toward astaxanthin, and to enhance its final titers while minimizing intermediate ketocarotenoid accumulation. We designed high-cell-density cultivations under optimized conditions, which can permit robust, photoautotrophic astaxanthin production in this green alga.

RESULTS AND DISCUSSION

Astaxanthin Accumulation in *C. reinhardtii* Does Not Interfere with Growth but Reduces Cellular Chlorophyll and Carotenoid Contents. Initial ketocarotenoid biosynthesis was established in *C. reinhardtii* UVM4 by the expression of a synthetically optimized *Cr*BKT[19] fused directly with an antibiotic resistance marker (aminoglycoside adenylyltransferase, aadA, Figure 1A). All recovered transformants exhibited the colored phenotype previously observed for *Cr*BKT expression, indicating substantial ketocarotenoid accumulation in vegetative *C. reinhardtii*.[19,41] Five randomly selected candidate transformants were isolated for subsequent characterization. It was observed that their growth was comparable to UVM4 parental strain under mixotrophic conditions (Figure 1B). However, total cellular chlorophyll and carotenoid contents were reduced by 29 ± 5% and 29 ± 4%, respectively (Figure 1C), in line with previous observations in *C. reinhardtii*[28] and tobacco chloroplasts expressing *Cr*BKT.[42] The functional expression of *Cr*BKT results in the biosynthesis of astaxanthin from zeaxanthin, accompanied by the conversion of ß-carotene into canthaxanthin in *C. reinhardtii*.[16,19] It is likely that altered pigment profiles in thylakoid membranes interfere with photosystem biogenesis and stability. In addition, feedback inhibition of ketocarotenoid formation could reduce cellular pigment levels.[43,44] Altered pigmentation (Figure 1), including reduced chlorophyll contents, can affect cellular photosynthetic efficiency or light penetration into the culture. Here, however, no effect on relative growth rates was observed. Under high-light conditions, the presence of high ketocarotenoid amounts was shown to increase photosynthetic parameters such as light-dependent oxygen evolution, relative electron transport rate, and elevated resistance to photoinhibition.[28]

Non-native pigment accumulation was visualized after 72 h mixotrophic cultivation via absorbance spectra determination and thin-layer chromatography (TLC) (Figure 1D,E). In acetone extracts, endogenous pigments exhibit two main peak maxima at 433 and 459 nm and absorbance rapidly decreases from 500 nm onward. *Cr*BKT enzyme activity resulted in an extended absorbance signal at ∼530 nm for all analyzed transformants, which represents a simple indicator for ketocarotenoid accumulation. In TLC, three distinct, red-orange-colored bands were detected, which were not present in parental strain UVM4 representing ketocarotenoid products from *Cr*BKT activity (e.g., astaxanthin, canthaxanthin, as well as intermediates). HPLC measurements of cellular extracts confirmed accumulation of approx. 0.8 mg L^{-1} astaxanthin and 5 mg L^{-1} canthaxanthin, respectively (Figure 2). Typically, nuclear transgenes in *C. reinhardtii* exhibit highly variable expression rates across a transformant population due to integration via nonhomologous end joining (NHEJ) into chromosome positions, which underlay individual aspects of eukaryotic gene expression regulation. When fused to the selection marker aadA, all regenerated transformants exhibited highly comparable colorimetric phenotypes, and little variation was observed across the tested transformants. These findings suggest that *Cr*BKT is highly active and is able to function to maximal capacity across variable expression levels. This observation suggested that ketocarotenoid production and cellular astaxanthin accumulation are likely not limited by the *Cr*BKT enzyme titer as it has been shown for other catalytically active enzymes in this host. In all strains, astaxanthin was not the major ketocarotenoid present, and residual ß-carotene levels were observed in analyzed transformants (Figure 1E, top bands), likely due to its essential roles in photosystem architecture, energy transfer, and singlet oxygen quenching.[45] Both factors indicate that further investigations of possible pathway limitations and metabolic engineering would be

https://doi.org/10.1021/acssynbio.2c00616
ACS Synth. Biol. 2023, 12, 820−831

required to channel intermediates toward astaxanthin as a final product.

Identifying Rate-Limiting Enzymes in Algal Astaxanthin Biosynthesis. The plastid-located MEP pathway in *C. reinhardtii* (Figure 2A) is an exceptional source of sustainable metabolites[33,36,46] and provides abundant precursor GGPP as a substrate for phytoene, phytyl diphosphate, and solanesyl diphosphate synthases. The carbon flux through the MEP pathway is reported to be limited by DXS and GGPPS as key enzymatic bottlenecks, which can be deregulated in *C. reinhardtii* by heterologous overexpression.[33,39,47] Sufficient GGPP levels are essential for phytol tail provision in chlorophyll biosynthesis and carotenoid production via phytoene synthase (PSY/crtB) activity, which plays important roles in light harvesting and protection. Engineered PSY/crtB overexpression has been reported to result in increased total carotenoid contents and enhanced photosynthetic capacities in plants and algae.[48−51] In addition, engineered PSY/crtB activity can induce chromoplast-like plastids differentiation including global gene expression reprogramming in tobacco.[50] Although engineering the precursor supply for carotenoid production is a common strategy for astaxanthin accumulation in several organisms,[13,48,52] such attempts have not yet been conducted in *C. reinhardtii*.

Two competing lycopene cyclases (LCYB and LCYE) balance the proportion of α- and ß-carotene after the cyclization of lycopene to contain ε-β or β-ionone-type end groups, respectively. In plants, flux toward ß-carotene can be enhanced by LCYB overexpression, which results in increased biomass, carotenoid contents, and improved stress tolerance[53−55] partially due to the deregulation of abscisic acid (ABA) biosynthesis and regulatory feedback effects. Hydroxylation and ketolation steps, involving the ß-carotene hydroxylase (CHYB) and ß-carotene ketolase (BKT), complete astaxanthin biosynthesis from ß-carotene.[8,9] In *C. reinhardtii*, the native expression of a CHYB is required for the xanthophyll cycle, which plays a key role in energy dissipation by nonphotochemical quenching.[56] *Cr*BKT expression resulted in increased xanthophyll and reduced chlorophyll a contents in transformed *S. lycopersiucum*[57,58] and increased high-light and temperature tolerance in *A. thaliana*,[59] respectively. The recombinant overexpression of other carotenoid pathway enzymes has not yet been performed in *C. reinhardtii*, and in this study, we investigated their effect in ketocarotenoid accumulating, *Cr*BKT-expressing transformant (BKT1, Figure 1).

We designed transgene constructs to allow the overexpression of different potentially rate-limiting enzymes of the carotenoid biosynthesis pathway in a *Cr*BKT-expressing *C. reinhardtii* strain (Figure 2B). Transgene sequences were derived from the current literature and included the fusion of target enzymes to a yellow fluorescent protein (YFP, mVenus) for rapid transformant identification and expression quantification in a population of 288 randomly isolated transformants. The fluorescence intensity was quantified for the 20 best-performing candidates (Figure 2C), and respective pigment quantification was performed by HPLC from pooled samples in technical triplicates (Figure 2D). Astaxanthin titers observed in most analyzed transformants were comparable to the *Cr*BKT-expressing parental control strain P1 and resulted in approx. 0.8 mg L^{-1} after 72 h of cultivation in mixotrophic conditions (Figure 2). Yields of other isoprenoid targets have been improved by subsequent transformations to increase catalytic enzyme titers in *C. reinhardtii*.[31−33,39,40,60] However, the production of astaxanthin was not increased by an elevated copy number of *Cr*BKT-expressing units in double transformants (Figure 2D, +BKT), further confirming the earlier observation of consistently colored phenotypes across the transformation population. *Cr*BKT likely has a high turnover rate, and astaxanthin production in *C. reinhardtii* is rather limited by a factor beyond the ketolation capacity of this enzyme, which encourages further investigation of metabolic engineering possibilities.

In previous reports, the engineered overexpression of DXS and GGPPS had a strong effect on heterologous diterpenoid production in *C. reinhardtii* but did not alter carotenoid biosynthesis even when significant amounts of GGPP were diverted to heterologous products.[33,40] As astaxanthin is a terminal carotenoid, its production may be influenced by rates of substrate availability derived from isoprenoid precursors for the carotenoid pathway. Here, the overexpression of either DXS or GGPP did not change the total carotenoid production and had no effect on astaxanthin titers in the *Cr*BKT-expressing line, suggesting that isoprenoid precursor availability was not a limiting factor in ketocarotenoid accumulation or its conversion to astaxanthin in *C. reinhardtii*. The overexpression of a heterologous phytoene synthase from a pigmented bacterium (*Pa*crtB) resulted in increased total carotenoid contents and increased canthaxanthin accumulation in the *Cr*BKT-expressing strain: 9.3 mg L^{-1} compared to 5.0 mg L^{-1} canthaxanthin in the parental control, but was not accompanied by a higher astaxanthin level (Figure 2D). Canthaxanthin is derived from ß-carotene by the addition of keto groups on both terminal rings. The increase of canthaxanthin, but not astaxanthin, caused by *Pa*crtB expression indicates that an increased flux toward carotenoids can be achieved and that the oxidation activity of *Cr*BKT is sufficient to utilize increased precursor availability. However, terminal hydroxylation to astaxanthin is still limited.

A 6.2-fold increase of astaxanthin to 5 mg L^{-1} and a drop in canthaxanthin levels to 0.7 mg L^{-1} were observed when *Cr*CHYB was coexpressed in the *Cr*BKT transformant (Figure 2D). These results suggest that endogenous ß-carotene hydroxylase activity is a present limitation in astaxanthin biosynthesis in *C. reinhardtii*. Previous studies relied on the use of heterologous ß-carotene hydroxylases,[61,62] which were shown to function in *C. reinhardtii*. However, our data confirm the hydroxylase activity of the predicted *Cr*CHYB and demonstrate its effectiveness to increase astaxanthin accumulation. Endogenous CHYB activity is highly regulated to balance xanthophyll biogenesis in green microalgae, however, genetic redesign of the coding sequence enabled effective *Cr*CHYB deregulation in this study. The strong metabolic effects observed from the overexpression of either *Cr*CHYB or *Pa*crtB were also consistent with the relative expression rates of these transgenes observed by high YFP fluorescence signals when normalized to optical densities (Figure 2C).

Combinatorial Overexpression of Rate-Limiting Enzymes. The combinatorial overexpression of *Cr*BKT, *Pa*crtB, and *Cr*CHYB was achieved by a third transformation of a CHYB_RFP fusion protein-expressing plasmid with nourseothricin selection in a *Cr*BKT+*Pa*crtB transformant (Figure 3A). Strains generated from this transformation allowed a comparison of effects from the expression of *Cr*BKT alone with double transformants expressing *Cr*BKT+*Pa*crtB and triple transformants with *Cr*BKT+*Pa*crtB+*Cr*CHYB. Initial

https://doi.org/10.1021/acssynbio.2c00616
ACS Synth. Biol. 2023, 12, 820−831

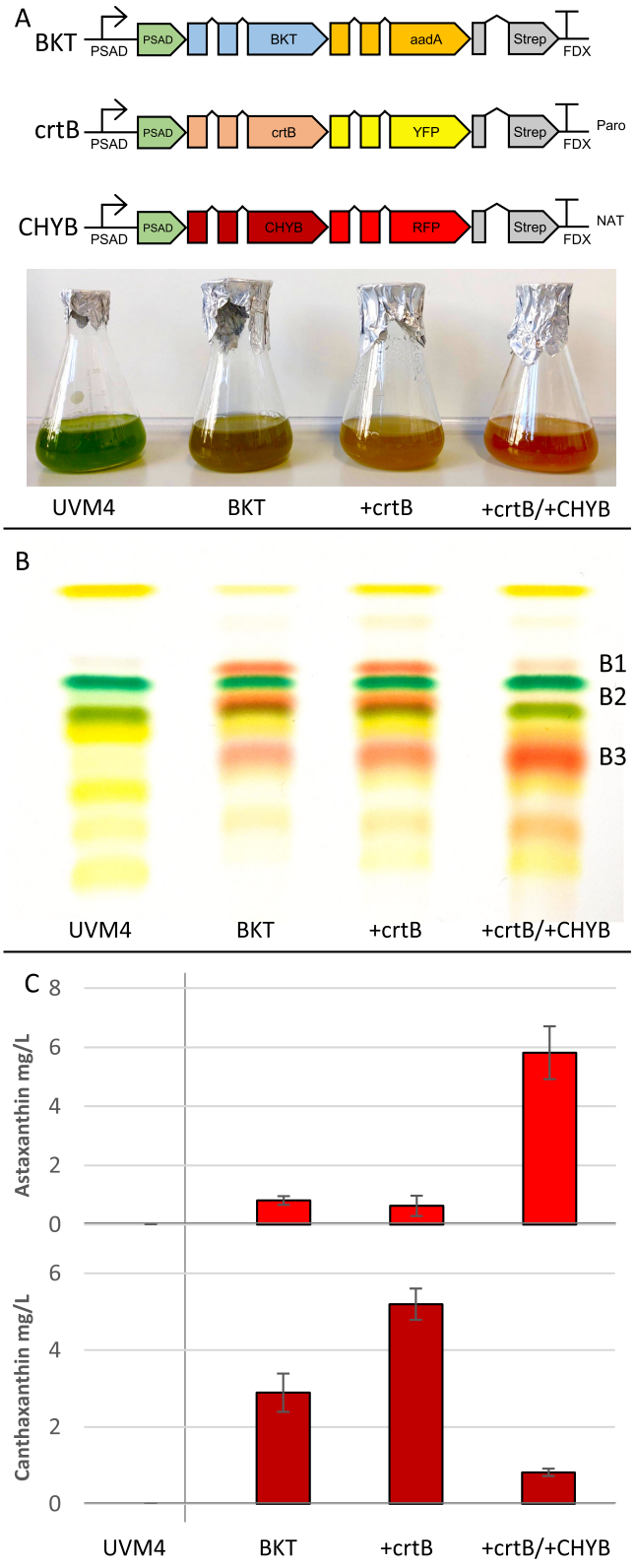

Figure 3. Gene design and combinatorial engineering for improved astaxanthin production. Coding sequences were designed to result in fusion proteins to either the selection marker aadA, the yellow fluorescence protein (mVenus, YFP), or red fluorescence reporter (mRuby2, RFP), as well as PSAD-targeting peptide and StrepII-tag. Transcription was driven by the PSAD promoter and the FXD1 terminator. Transformations using plasmids coding for fluorescence protein fusion constructs were performed along with a selection marker expression construct (Paro, NAT). Representative culture flasks after 120 h of mixotrophic cultivations of UVM4 and respective transformants are depicted below. (B) Thin-layer chromatography of acetone extracts from *C. reinhardtii* UVM4 culture, a BKT-expressing transformant (BKT), and strains coexpressing either *P. ananatis* phytoene desaturase (+crtB) or *P. ananatis* phytoene desaturase and *C. reinhardtii* ß-carotene 3-hydroxylase (+crtB/+CHYB) from subsequent transformations. (C) Quantification of volumetric canthaxanthin and astaxanthin production after 72 h of mixotrophic cultivations. Results represent mean values and standard deviation from biological triplicates (n = 3).

astaxanthin production by *Cr*BKT expression in *C. reinhardtii* UVM4 resulted in 0.81 mg L^{-1} astaxanthin and 2.9 mg L^{-1} canthaxanthin after 72 h of mixotrophic cultivation and three distinctly colored bands in thin-layer chromatography (B1−B3, Figure 3B). Canthaxanthin levels were slightly reduced compared to previous experiments (Figure 2D), likely due to changes in cultivation regimes (Erlenmeyer flasks compared to 24-well microtiter plates) with reduced light availability. Light intensity strongly affects cellular carotenoid contents in plants and algae.[63−66] The overexpression of *Pa*crtB resulted in a metabolic push through the carotenoid pathway from phytoene and a 79% increase in canthaxanthin levels in the *Cr*BKT background (5.2 mg L^{-1}, Figure 3C). The expression of CHYB in the *Cr*BKT+*Pa*crtB background led to a reduction of canthaxanthin to 0.8 mg L^{-1} and a 7.2-fold increase in astaxanthin accumulation from 0.81 mg L^{-1} to 5.82 mg L^{-1} (Figure 3C), 16% higher compared to *Cr*CHYB expression in the *Cr*BKT line alone (Figure 2D) under respective conditions. In TLC, the signal intensities of bands B1 and B2 were strongly decreased, while the presence of B3 was strongly increased in this strain, likely representing canthaxanthin or echinenone and astaxanthin, respectively (Figure 3B).

Our results suggest that *Pa*crtB overexpression can encourage an increased flux toward ß-carotene, and indicate that the hydroxylation of ß-carotene as well as canthaxanthin are limiting steps in astaxanthin biosynthesis in *C. reinhardtii*. The initial protein titers produced by *Cr*BKT single transgene expression were able to act on all intermediates available, and our work demonstrates higher astaxanthin accumulation when precursor limitations were removed by *Pa*crtB or *Cr*CHYB overexpression (Figures 2D, 3). Our findings suggest that *Cr*BKT has a high turnover rate and that the algal cell has a high astaxanthin accumulation capacity when hydroxylation can meet the rate of precursor oxidation.

A comparable coexpression experiment has been previously performed by heterologously expressing ß-carotene ketolase and ß-carotene hydroxylase from *H. lacustris* in *C. reinhardtii* CC-849.[67] Although it remains elusive why astaxanthin accumulation was already detected in the wild type in the respective study, a 34% gravimetric increase was observed for transformant cell lines. This is in line with our findings and corroborates the synergistic effect of increased ß-carotene hydroxylase activity on both zeaxanthin and canthaxanthin. However, the application of innovative gene design, use of suitable cell lines and sophisticated metabolic engineering, outperforms previously reported yields and demonstrates the great potential of *C. reinhardtii* as green cell factories.

Phototrophic Cultivation Increases Volumetric Astaxanthin Accumulation. The cultivation of the triple transformant (*Cr*BKT, *Pa*crtB, *Cr*CHYB) in mixotrophic (TAP)

https://doi.org/10.1021/acssynbio.2c00616
ACS Synth. Biol. 2023, 12, 820−831

and photoautotrophic (T2P) conditions followed a similar, sigmoidal pattern with a pronounced growth phase from 24 to 48 h post inoculation and a subsequent transition into stationary growth phase (Figure 4A). Both cultures reached 5.5×10^7 cells mL^{-1} after 72 h and 2.2 g L^{-1} and 2.1 g L^{-1} final cell dry weight (CDW), respectively. Volumetric production of astaxanthin increased during the culture growth phase and resulted in 8.6 ± 0.3 mg L^{-1} after 72 h for both mixotrophic and photoautotrophic cultivations. Maximal volumetric production was achieved in a TAP medium after 120 h with 9.5 ± 0.3 mg L^{-1} astaxanthin and 1.6 ± 0.3 mg L^{-1} canthaxanthin. Photoautotrophic cultivation likely suffers from nitrogen limitation typically associated with pigment reduction and protein degradation[32] and exhibits slightly reduced astaxanthin contents at later time points. In addition, established high cell densities limit penetration of light into a bioreactor, inducing a reduction of total carotenoid contents. Finally, the prolonged high light application can lead to the loss of the product by pigment oxidation,[68] which characterizes earlier time points with efficient space/time yields as suitable for economic production. Specific productivities under applied cultivation conditions resulted in 4.5 mg g^{-1} CDW, which is comparable to values from heterotroph chassis, e.g., 7.8 mg g^{-1} CDW astaxanthin in *E. coli* after 60 h of fed-batch fermentation[11] and 3.1 mg g^{-1} CDW in *C. glutamicum* after 48 h of batch cultivation.[13] Eukaryotic cell membrane structures and high enzymatic activity of endogenous *Cr*BKT and *Cr*CHYB in combination with sophisticated genetic tools are likely factors for successful astaxanthin production in *C. reinhardtii* and demonstrate the great biotechnological potential of eukaryotic microalgae.

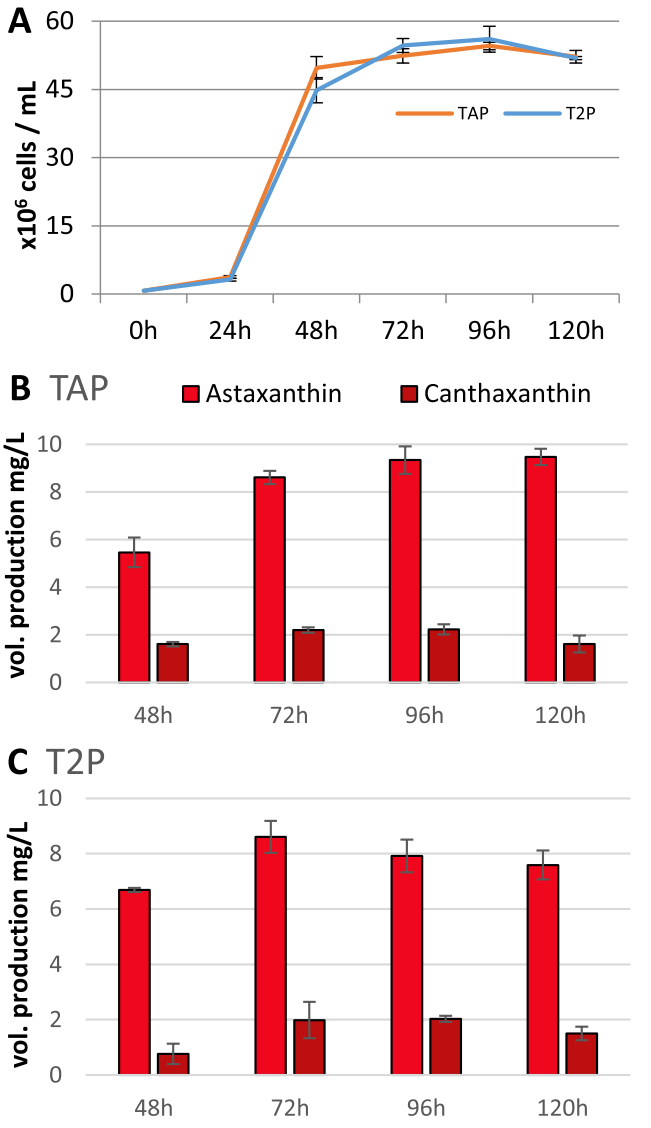

Figure 4. Cultivation of the production strain derived from transformations with *Cr*BKT, *Pac*rtB, and *Cr*CHYB. (A) Cell counts during the course of cultivation in mixotrophic conditions (TAP) and photoautotrophic (T2P) conditions in stirred Erlenmeyer flasks using 350 mL of the culture volume. Both cultures were provided with 5% (v/v) CO_2-enriched air and 500 μmol photons m^{-2} s^{-1}, which were increased to 850 μmol photons m^{-2} s^{-1} after 72 h. Results represent mean values and standard deviation from biological triplicates (n = 3). (B) Volumetric astaxanthin and canthaxanthin contents at indicated time points during mixotrophic cultivation. Results represent mean values and standard deviation from biological triplicates (n = 3). (C) Volumetric astaxanthin and canthaxanthin contents at indicated time points during photoautotrophic cultivations. Results represent mean values and standard deviation from biological triplicates (n = 3).

High-Light and High-Cell-Density Cultivation. A major limitation to algal production concepts has previously been the low volumetric cell densities associated with phototrophic growth compared to microbial fermentation counterparts. Recently established high-cell-density cultivations[32,69] are powerful strategies to overcome the generally low cell densities in microalgal cultivations limiting volumetric product yields. Here, the application of high-light assists in sufficient energy provision when light penetration is low. It has also been shown that short-term high-light application can increase cellular carotenoid accumulation in algae,[65,70,71] and the application of high-light is combined with high cell density cultivations in this study. Nitrate utilization capability was restored in an engineered production strain (*Cr*BKT, *Pac*rtB, and *Cr*CHYB) by complementation of genomic nitrate reductase (NIT1) and nitrate assimilation regulatory protein (NIT2), and cultivations were performed in an airlift photobioreactor using 6xP medium[32] subjected to a constant stream of 3% CO_2-enriched air and to very high light (3,000 μmol photons m^{-2} s^{-1}). The astaxanthin-accumulating algal cells were able to tolerate this extreme high light, reinforcing the role of this pigment in photoprotection.[28] The stationary growth phase was reached at an optical density of 1.8 after 94 h (Figure 5). Maximal volumetric astaxanthin production (Figure 5A) was observed to be 23.5 mg L^{-1} after 94 h in 6xP medium, which displays the highest reported non-native ketocarotenoid accumulation from a green microalga. Volumetric astaxanthin productivity, correlated with the algal growth phase with a reduction during the stationary growth phase, resulted in 0.29 mg L^{-1} h^{-1} on average throughout the entire cultivation and peaked between 54 and 56 h sampling points with maximal 1.09 mg L^{-1} h^{-1} (Figure 5B). Astaxanthin productivities from *H. lacustris* have been reported to range between 0.12 and 15 mg L^{-1} day^{-1},[72,73] while 2.8 mg L^{-1} day^{-1} was achieved in engineered *Synechocystis*[74] and 37.5 mg L^{-1} day^{-1} in engineered yeast under heterotrophic conditions.[75] The volumetric productivity achieved in this study (25 mg L^{-1} day^{-1}) solely relies on the utilization of CO_2 as the only carbon source and displays a competitive and sustainable alternative compared to other astaxanthin production platforms.

This work identified key enzymatic bottlenecks in carotenoid biosynthesis in *C. reinhardtii* and provided

https://doi.org/10.1021/acssynbio.2c00616
ACS Synth. Biol. 2023, 12, 820−831

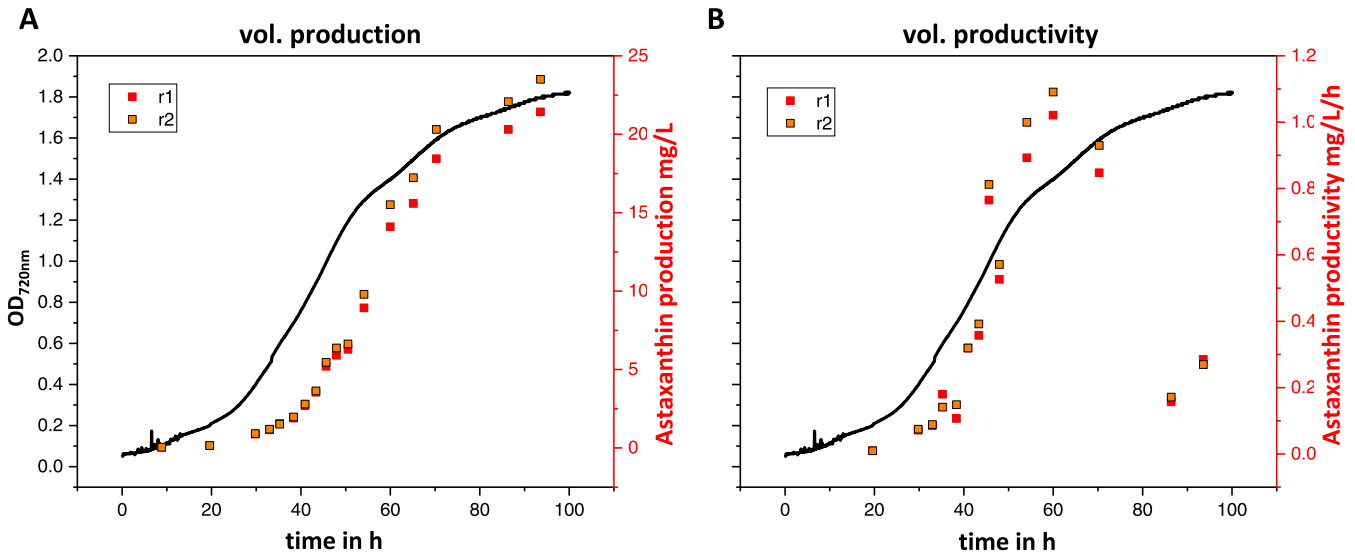

Figure 5. High-cell-density cultivation under very high light of an engineered production strain (*Cr*BKT, *Pac*rtB, *Cr*CHYB, and Nit1/2). Cultivations were performed using a 6xP medium[32] in a Multi-Cultivator MC-1000 (Photon Systems Instruments) at 3000 μmol photons m^{-2} s^{-1}, 24 °C, and a constant stream of 3% (v/v) CO_2-enriched air. (A) Volumetric production and optical density measurements at 720 nm. (B) Volumetric productivity and optical density measurements at 720 nm. Results represent measurements from two biological replicates (r1, r2).

advanced strategies for repartitioning substantial carbon toward ketocarotenoid products. The application of potent genetic engineering strategies in combination with optimized photoautotrophic cultivation regimes demonstrates the great potential of *C. reinhardtii* as a green cell factory.

MATERIAL AND METHODS

Genetic Constructs and Plasmid Design. Plasmids were designed using pOptimized vectors[39,76,77] with the following modifications: all expression elements were placed under the transcriptional control of the *C. reinhardtii* PSAD promoter including the 5′UTR[78] and FDX1 terminator[29] and carried the N-terminal PSAD chloroplast transit peptide (CTP).[78]

The *C. reinhardtii* BKT (UniProt: Q4VKB4)[19] was inserted at the N-terminus of the aadA-reporter in a pOpt2_MinS construct (BKT_aadA, Figure 1). The coding sequences of a *Salvia pomifera* 1-deoxy-D-xylulose-5-phosphate synthase 2 mutant variant (DXS, NCBI: MH178297), *Pantoea ananatis* phytoene synthase (crtB, UniProt: D4GFK9), *C. reinhardtii* geranylgeranyl pyrophosphate synthase (GGPPS, UniProt: A8JHU6), *Daucus carota* lycopene β cyclase (LCYB, UniProt: A0A164WPY9), and *C. reinhardtii* β-carotene 3-hydroxylase (CHYB, UniProt: Q4VKB5) were redesigned to carry multiple copies of RBCS2i1 and to match the *C. reinhardtii* codon usage, as previously described[25] using Intronserter.[26] Commercially synthesized coding sequences (Genscript) of *Cr*BKT, *Pac*rtB, *Dc*LCYB, and *Cr*CHYB were inserted at the N-terminus of the mVenus reporter construct in pOpt3_PSAD_mVenus_Paro[27](Figure 2). All reporter constructs (aadA, mVenus, and mRuby) were redesigned to contain two copies of RBCS2i1 in suitable insertion sites[25] and to carry a C-terminal RBCS2i2 including a StrepII-tag, as previously described.[27]

The *Cr*GGPPS was PCR amplified (Q5 Polymerase, NEB) according to the manufacturer's protocol to carry an ochre stop codon and was inserted at the C-terminus of the mVenus reporter in pOpt3_PSAD_mVenus_Paro and pOpt3_PSAD_crtB_mVenus_Paro to facilitate product channeling, as previously described (Figure 2).[40] *Cr*CHYB was additionally inserted at the N-terminus of the mRuby2 reporter in a pOpt3_mRuby_NAT construct carrying the nourseothricin acetyltransferase resistance gene (Figure 3).[79]

All cloning was performed by digestions with respective restriction enzymes (*BamHI/BglII* or *EcoRV/EcoRI*, NEB), followed by DNA extraction after gel electrophoreses (peqGOLD gel extraction kit, VWR) and ligation (T4 Ligase, NEB) according to the manufacturer's protocol. Ligation products were used for heat shock transformation of chemically competent DH5a cells and selection on LB agar plates containing ampicillin (300 mg L^{-1}). Plasmid isolation was performed using the peqGold plasmid isolation kit (VWR) according to the manufacturer's protocol. Sequence identity was confirmed by Sanger sequencing (Sequencing Core Facility, CeBiTec, Bielefeld University).

***C. reinhardtii* Transformation and Selection.** Strain *C. reinhardtii* UVM4[80] was routinely maintained at room temperature on TAP agar plates[81] with modified micronutrient contents[82] and cultivated in Erlenmeyer flasks using liquid media and constant light at 350 μmol photons m^{-2} s^{-1}.

The nuclear transformation was carried out by glass bead agitation[83] using 10 μg of linearized plasmid DNA (*XbaI/KpnI*, NEB), followed by regeneration for 8−16 h at 25 μmol photons m^{-2} s^{-1} prior to plating on TAP agar plates containing respective antibiotics (200 mg L^{-1} spectinomycin, 10 mg L^{-1} paromomycin, or 2.5 mg L^{-1} nourseothricin). For systematic comparisons, 288 transformants were isolated from the regenerated transformant populations. Of these, the best 20 expressing transformants were identified using fluorescence measurements in a plant imaging system (NightShade LB 985, Berthold technologies) with appropriate filter sets for mVenus (excitation: 504 nm, emission: 530 nm) and mRuby2 (excitation: 560 nm, emission: 600 nm). Transformants were individually cultivated in microtiter plates and pooled samples were used for pigment quantification.

The best-performing transformant derived from the iterative transformation of UVM4 with constructs pOpt3_PSAD_BKT_aadA, pOpt3_PSAD_crtB_mVenus_Paro, and pOpt3_-

https://doi.org/10.1021/acssynbio.2c00616
ACS Synth. Biol. 2023, 12, 820−831

PSAD_CHYB_RFP_NAT was directly identified by fluorescence microscopy (Leica MZ FLIII, Leica Microsystems) using appropriate filter sets for mVenus (excitation: 510/20 nm, emission: 560/40 nm) and mRuby2 (excitation: 545/30 nm, emission: at 620/60 nm). The nitrate capability of *C. reinhardtii* strains was complemented by transformation with pMN24 and pMN68, as previously described.[40]

Microalgal Cultivation. Isolated transformants were cultivated individually in microtiter plates or Erlenmeyer flasks using a TAP medium without antibiotics on an orbital shaker (GFL, 30 mm amplitude, 120−180 rpm) and at constant illumination of 350−500 μmol photons m^{-2} s^{-1} at room temperature. After 72 h, the light intensity was increased to 850 μmol photons m^{-2} s^{-1} to provide sufficient illumination. Cultivations under phototrophic conditions were performed in stirred Erlenmeyer flasks using 350 mL of a T2P medium,[39] and where indicated, a constant stream of 5% (v/v) CO_2-enriched air was applied.

High-light cultivations were performed in a 6xP medium[32] using a Multi-Cultivator MC-1000 (Photon Systems Instruments) at 3000 μmol photons m^{-2} s^{-1}, 24 °C and a constant stream of 3% (v/v) CO_2-enriched air. Growth was continuously monitored via optical density (OD) measurements at 720 nm.

Cell densities were quantified using a Z2 Particle Counter (Beckman Coulter Life Sciences) or a Countess II FL Automated Cell Counter (Thermo Fisher Scientific). The cell dry weight (CDW) was gravimetrically determined from 5−10 mL of culture pellets after centrifugation at 3000*g* for 5 min and drying overnight at 105 °C.

Absorbance Spectrum, Pigment Quantification, and Thin-Layer Chromatography. Absorbance spectra from 350 to 750 nm were recorded for acetone extracts from cell culture pellets in a NanoDrop One photometer, and total pigments were determined as previously described.[39] Thin-layer chromatography was performed with concentrated acetone extracts from cell pellets and separated on silica gel plates (Nano-ADAMANT 0.2 mm, Macherey and Nagel) using an appropriate running buffer (89.5% (v/v) petroleum, 10% (v/v) isopropanol, 0.5% (v/v) water).

High-performance liquid chromatography (HPLC) was performed as previously described.[13] Briefly, an Agilent 1200 series system (Agilent Technologies), equipped with a C18 reverse-phase column (LiChrospher 100 RP18 EC-5, 125 mm × 4 mm) and a precolumn (LiChrospher 100 RP18 EC-5, 40 mm × 4 mm), was used with a diode array detector measuring at a wavelength of 470 nm. Carotenoids were separated using a gradient between 9:1 methanol:water (A) and methanol (B) at 1.5 mL min^{-1} in gradient: 0 min B: 0%, 10 min B: 100%, 32.5 min B: 100%, and 33 min B: 0%.

High-performance liquid chromatography (HPLC) for samples from high-light cultivations (Figure 5) was performed as previously described.[19] Briefly, a Jasco Extrema LC-4000 HPLC system and a C18 reverse-phase column (Synergy Hydro-RP, Phenomenex) were used with an ethyl acetate gradient (0−100%) in an acetonitrile−water−triethylamine solution (9:1:0.01) at a flow rate of 1.5 mL min^{-1}. Pigment detection was conducted with a 350−750 nm diode array detector. Identification and quantification of chromatogram signals were compared to commercially available authentic standards (CaroteNature GmbH, Sigma, Extrasynthese, VWR).

AUTHOR INFORMATION

Corresponding Author

Thomas Baier − *Algae Biotechnology and Bioenergy, Faculty of Biology, Center for Biotechnology (CeBiTec), Bielefeld University, 33615 Bielefeld, Germany;* orcid.org/0000-0002-5226-3035; Phone: +49 521 106-12289; Email: thomas.baier@uni-bielefeld.de; Fax: +49 521 106-12290

Authors

Sofia Amendola − *Algae Biotechnology and Bioenergy, Faculty of Biology, Center for Biotechnology (CeBiTec), Bielefeld University, 33615 Bielefeld, Germany*

Jacob S. Kneip − *Algae Biotechnology and Bioenergy, Faculty of Biology, Center for Biotechnology (CeBiTec), Bielefeld University, 33615 Bielefeld, Germany;* orcid.org/0000-0001-7384-5934

Florian Meyer − *Genetics of Prokaryotes, Faculty of Biology, Center for Biotechnology (CeBiTec), Bielefeld University, 33615 Bielefeld, Germany*

Federico Perozeni − *Department of Biotechnology, University of Verona, 37129 Verona, Italy*

Stefano Cazzaniga − *Department of Biotechnology, University of Verona, 37129 Verona, Italy*

Kyle J. Lauersen − *Bioengineering Program, Biological and Environmental Sciences and Engineering Division, King Abdullah University of Science and Technology (KAUST), Thuwal 23955, Kingdom of Saudi Arabia;* orcid.org/0000-0002-5538-7201

Matteo Ballottari − *Department of Biotechnology, University of Verona, 37129 Verona, Italy;* orcid.org/0000-0001-8410-3397

Complete contact information is available at: https://pubs.acs.org/10.1021/acssynbio.2c00616

Funding

This research was supported by the ERC Starting Grant SOLENALGAE (679814) and the University of Verona grant no. JPVR2018BALLOTTARI to M.B. Funding to K.J.L. was provided by the King Abdullah University of Science and Technology (KAUST) baseline research funding. F.M. acknowledges funding by BMBF project KaroTec (grant number: 03VP09460).

Notes

The authors declare no competing financial interest.

ACKNOWLEDGMENTS

The authors would like to express their thanks to Prof. Dr. Ralph Bock for providing strain UVM4 and to Tim Prausner for performing TLC.

REFERENCES

(1) Shah, M. M. R.; Liang, Y.; Cheng, J. J.; Daroch, M. Astaxanthin-Producing Green Microalga Haematococcus Pluvialis: From Single Cell to High Value Commercial Products. *Front. Plant Sci.* **2016**, *7*, No. 531.

(2) Li, X.; Wang, X.; Duan, C.; Yi, S.; Gao, Z.; Xiao, C.; Agathos, S. N.; Wang, G.; Li, J. Biotechnological Production of Astaxanthin from the Microalga Haematococcus Pluvialis. *Biotechnol. Adv.* **2020**, *43*, No. 107602.

(3) Wan, X.; Zhou, X.-R.; Moncalian, G.; Su, L.; Chen, W.-C.; Zhu, H.-Z.; Chen, D.; Gong, Y.-M.; Huang, F.-H.; Deng, Q.-C.

Reprogramming Microorganisms for the Biosynthesis of Astaxanthin via Metabolic Engineering. *Prog. Lipid Res.* **2021**, *81*, No. 101083.
(4) Zhang, C.; Chen, X.; Too, H.-P. Microbial Astaxanthin Biosynthesis: Recent Achievements, Challenges, and Commercialization Outlook. *Appl. Microbiol. Biotechnol.* **2020**, *104*, 5725−5737.
(5) Seybold, A.; Goodwin, T. W. Occurrence of Astaxanthin in the Flower Petals of Adonis Annua L. *Nature* **1959**, *184*, 1714−1715.
(6) Dixon, C.; Wilken, L. R. Green Microalgae Biomolecule Separations and Recovery. *Bioresour. Bioprocess.* **2018**, *5*, No. 14.
(7) Latowski, D.; Kuczyńska, P.; Strzałka, K. Xanthophyll Cycle − a Mechanism Protecting Plants against Oxidative Stress. *Redox Rep.* **2011**, *16*, 78−90.
(8) Cunningham, F. X.; Gantt, E. Genes and Enzymes of Carotenoid Biosynthesis in Plants. *Annu. Rev. Plant Physiol. Plant Mol. Biol.* **1998**, *49*, 557−583.
(9) Lotan, T.; Hirschberg, J. Cloning and Expression in *Escherichia coli* of the Gene Encoding *β*-C-4-Oxygenase, That Converts *β*-Carotene to the Ketocarotenoid Canthaxanthin in Haematococcus Pluvialis. *FEBS Lett.* **1995**, *364*, 125−128.
(10) Park, S. Y.; Binkley, R. M.; Kim, W. J.; Lee, M. H.; Lee, S. Y. Metabolic Engineering of *Escherichia coli* for High-Level Astaxanthin Production with High Productivity. *Metab. Eng.* **2018**, *49*, 105−115.
(11) Gong, Z.; Wang, H.; Tang, J.; Bi, C.; Li, Q.; Zhang, X. Coordinated Expression of Astaxanthin Biosynthesis Genes for Improved Astaxanthin Production in *Escherichia coli*. *J. Agric. Food Chem.* **2020**, *68*, 14917−14927.
(12) Henke, N.; Heider, S.; Peters-Wendisch, P.; Wendisch, V. Production of the Marine Carotenoid Astaxanthin by Metabolically Engineered *Corynebacterium glutamicum*. *Mar. Drugs* **2016**, *14*, 124.
(13) Henke, N. A.; Wendisch, V. F. Improved Astaxanthin Production with *Corynebacterium glutamicum* by Application of a Membrane Fusion Protein. *Mar. Drugs* **2019**, *17*, 621.
(14) Zhou, P.; Ye, L.; Xie, W.; Lv, X.; Yu, H. Highly Efficient Biosynthesis of Astaxanthin in *Saccharomyces cerevisiae* by Integration and Tuning of Algal CrtZ and Bkt. *Appl. Microbiol. Biotechnol.* **2015**, *99*, 8419−8428.
(15) Zhu, X.; Meng, C.; Sun, F.; Wei, Z.; Chen, L.; Chen, W.; Tong, S.; Du, H.; Gao, J.; Ren, J.; Li, D.; Gao, Z. Sustainable Production of Astaxanthin in Microorganisms: The Past, Present, and Future. *Crit. Rev. Food Sci. Nutr.* **2022**, 1−17.
(16) Tran, N. T.; Kaldenhoff, R. Metabolic Engineering of Ketocarotenoids Biosynthetic Pathway in *Chlamydomonas Reinhardtii* Strain CC-4102. *Sci. Rep.* **2020**, *10*, No. 10688.
(17) Zhong, Y.-J.; Huang, J.-C.; Liu, J.; Li, Y.; Jiang, Y.; Xu, Z.-F.; Sandmann, G.; Chen, F. Functional Characterization of Various Algal Carotenoid Ketolases Reveals That Ketolating Zeaxanthin Efficiently Is Essential for High Production of Astaxanthin in Transgenic Arabidopsis. *J. Exp. Bot.* **2011**, *62*, 3659−3669.
(18) Lohr, M.; Im, C.-S.; Grossman, A. R. Genome-Based Examination of Chlorophyll and Carotenoid Biosynthesis in *Chlamydomonas reinhardtii*. *Plant Physiol.* **2005**, *138*, 490−515.
(19) Perozeni, F.; Cazzaniga, S.; Baier, T.; Zanoni, F.; Zoccatelli, G.; Lauersen, K. J.; Wobbe, L.; Ballottari, M. Turning a Green Alga Red: Engineering Astaxanthin Biosynthesis by Intragenic Pseudogene Revival in *Chlamydomonas reinhardtii*. *Plant Biotechnol. J.* **2020**, *18*, No. pbi.13364.
(20) He, J.; Li, P.; Huo, H.; Liu, L.; Tang, T.; He, M.; Huang, J.; Liu, L. Heterologous Expression of HpBHY and CrBKT Increases Heat Tolerance in Physcomitrella Patens. *Plant Diversity* **2019**, *41*, 266−274.
(21) Lin, Y.; He, M.; Wang, J.; Huang, J. Fruit-Specific Expression of CrtB, HpBHY, CrBKT and SlLCYB in a Special Tomato Landrace Triggers Hyper Production of Carotenoids in the Fruit. *J. Plant Biol.* **2021**, *64*, 447−459.
(22) Huang, J.-C.; Zhong, Y.-J.; Liu, J.; Sandmann, G.; Chen, F. Metabolic Engineering of Tomato for High-Yield Production of Astaxanthin. *Metab. Eng.* **2013**, *17*, 59−67.
(23) Bai, C.; Berman, J.; Farre, G.; Capell, T.; Sandmann, G.; Christou, P.; Zhu, C. Reconstruction of the Astaxanthin Biosynthesis Pathway in Rice Endosperm Reveals a Metabolic Bottleneck at the Level of Endogenous *β*-Carotene Hydroxylase Activity. *Transgenic Res.* **2017**, *26*, 13−23.
(24) Zhu, Q.; Zeng, D.; Yu, S.; Cui, C.; Li, J.; Li, H.; Chen, J.; Zhang, R.; Zhao, X.; Chen, L.; Liu, Y.-G. From Golden Rice to ASTARice: Bioengineering Astaxanthin Biosynthesis in Rice Endosperm. *Mol. Plant* **2018**, *11*, 1440−1448.
(25) Baier, T.; Wichmann, J.; Kruse, O.; Lauersen, K. J. Intron-Containing Algal Transgenes Mediate Efficient Recombinant Gene Expression in the Green Microalga *Chlamydomonas reinhardtii*. *Nucleic Acids Res.* **2018**, *46*, 6909−6919.
(26) Jaeger, D.; Baier, T.; Lauersen, K. J. Intronserter, an Advanced Online Tool for Design of Intron Containing Transgenes. *Algal Res.* **2019**, *42*, No. 101588.
(27) Baier, T.; Jacobebbinghaus, N.; Einhaus, A.; Lauersen, K. J.; Kruse, O. Introns Mediate Post-Transcriptional Enhancement of Nuclear Gene Expression in the Green Microalga *Chlamydomonas reinhardtii*. *PLOS Genet.* **2020**, *16*, No. e1008944.
(28) Cazzaniga, S.; Perozeni, F.; Baier, T.; Ballottari, M. Engineering Astaxanthin Accumulation Reduces Photoinhibition and Increases Biomass Productivity under High Light in *Chlamydomonas reinhardtii*. *Biotechnol. Biofuels Bioprod.* **2022**, *15*, No. 77.
(29) Einhaus, A.; Baier, T.; Rosenstengel, M.; Freudenberg, R. A.; Kruse, O. Rational Promoter Engineering Enables Robust Terpene Production in Microalgae. *ACS Synth. Biol.* **2021**, *10*, 847−856.
(30) Schroda, M. Good News for Nuclear Transgene Expression in Chlamydomonas. *Cells* **2019**, *8*, 1534.
(31) Freudenberg, R. A.; Wittemeier, L.; Einhaus, A.; Baier, T.; Kruse, O. Advanced Pathway Engineering for Phototrophic Putrescine Production. *Plant Biotechnol. J.* **2022**, *20*, 1968−1982.
(32) Freudenberg, R. A.; Baier, T.; Einhaus, A.; Wobbe, L.; Kruse, O. High Cell Density Cultivation Enables Efficient and Sustainable Recombinant Polyamine Production in the Microalga *Chlamydomonas reinhardtii*. *Bioresour. Technol.* **2021**, *323*, No. 124542.
(33) Einhaus, A.; Steube, J.; Freudenberg, R. A.; Barczyk, J.; Baier, T.; Kruse, O. Engineering a Powerful Green Cell Factory for Robust Photoautotrophic Diterpenoid Production. *Metab. Eng.* **2022**, *73*, 82−90.
(34) Freudenberg, R. A.; Wittemeier, L.; Einhaus, A.; Baier, T.; Kruse, O. The Spermidine Synthase Gene SPD1: A Novel Auxotrophic Marker for *Chlamydomonas reinhardtii* Designed by Enhanced CRISPR/Cas9 Gene Editing. *Cells* **2022**, *11*, 837.
(35) Schroda, M.; Remacle, C. Molecular Advancements Establishing Chlamydomonas as a Host for Biotechnological Exploitation. *Front. Plant Sci.* **2022**, *13*, No. 911483.
(36) Lauersen, K. J. Eukaryotic Microalgae as Hosts for Light-Driven Heterologous Isoprenoid Production. *Planta* **2019**, *249*, 155−180.
(37) Abdallah, M. N.; Wellman, G. B.; Overmans, S.; Lauersen, K. J. Combinatorial Engineering Enables Photoautotrophic Growth in High Cell Density Phosphite-Buffered Media to Support Engineered *Chlamydomonas reinhardtii* Bio-Production Concepts. *Front. Microbiol.* **2022**, *13*, No. 1337.
(38) Fields, F. J.; Lejzerowicz, F.; Schroeder, D.; Ngoi, S. M.; Tran, M.; McDonald, D.; Jiang, L.; Chang, J. T.; Knight, R.; Mayfield, S. Effects of the Microalgae Chlamydomonas on Gastrointestinal Health. *J. Funct. Foods* **2020**, *65*, No. 103738.
(39) Wichmann, J.; Baier, T.; Wentnagel, E.; Lauersen, K. J. K. J.; Kruse, O. Tailored Carbon Partitioning for Phototrophic Production of (E)-*α*-Bisabolene from the Green Microalga *Chlamydomonas reinhardtii*. *Metab. Eng.* **2018**, *45*, 211−222.
(40) Lauersen, K. J.; Wichmann, J.; Baier, T.; Kampranis, S. C.; Pateraki, I.; Møller, B. L.; Kruse, O. Phototrophic Production of Heterologous Diterpenoids and a Hydroxy-Functionalized Derivative from *Chlamydomonas reinhardtii*. *Metab. Eng.* **2018**, *49*, 116−127.
(41) Pivato, M.; Perozeni, F.; Licausi, F.; Cazzaniga, S.; Ballottari, M. Heterologous Expression of Cyanobacterial Orange Carotenoid Protein (OCP2) as a Soluble Carrier of Ketocarotenoids in *Chlamydomonas reinhardtii*. *Algal Res.* **2021**, *55*, No. 102255.

https://doi.org/10.1021/acssynbio.2c00616
ACS Synth. Biol. 2023, 12, 820−831

(42) Agrawal, S.; Karcher, D.; Ruf, S.; Erban, A.; Hertle, A. P.; Kopka, J.; Bock, R. Riboswitch-Mediated Inducible Expression of an Astaxanthin Biosynthetic Operon in Plastids. *Plant Physiol.* **2022**, *188*, 637−652.
(43) Chen, G.; Wang, B.; Han, D.; Sommerfeld, M.; Lu, Y.; Chen, F.; Hu, Q. Molecular Mechanisms of the Coordination between Astaxanthin and Fatty Acid Biosynthesis in Haematococcus Pluvialis (Chlorophyceae). *Plant J.* **2015**, *81*, 95−107.
(44) Schroeder, W. A.; Johnson, E. A. Singlet Oxygen and Peroxyl Radicals Regulate Carotenoid Biosynthesis in Phaffia Rhodozyma. *J. Biol. Chem.* **1995**, *270*, 18374−18379.
(45) Xu, P.; Chukhutsina, V. U.; Nawrocki, W. J.; Schansker, G.; Bielczynski, L. W.; Lu, Y.; Karcher, D.; Bock, R.; Croce, R. Photosynthesis without β-Carotene. *eLife* **2020**, *9*, No. e58984.
(46) Wichmann, J.; Lauersen, K. J.; Kruse, O. Green Algal Hydrocarbon Metabolism Is an Exceptional Source of Sustainable Chemicals. *Curr. Opin. Biotechnol.* **2020**, *61*, 28−37.
(47) Lauersen, K. J.; Wichmann, J.; Baier, T.; Kampranis, S. C.; Pateraki, I.; Møller, B. L.; Kruse, O. Phototrophic Production of Heterologous Diterpenoids and a Hydroxy-Functionalized Derivative from *Chlamydomonas reinhardtii*. *Metab. Eng.* **2018**, *49*, 116−127.
(48) Li, C.; Ji, J.; Wang, G.; Li, Z.; Wang, Y.; Fan, Y. Over-Expression of LcPDS, LcZDS, and LcCRTISO, Genes From Wolfberry for Carotenoid Biosynthesis, Enhanced Carotenoid Accumulation, and Salt Tolerance in Tobacco. *Front. Plant Sci.* **2020**, *11*, No. 119.
(49) Shewmaker, C. K.; Sheehy, J. A.; Daley, M.; Colburn, S.; Ke, D. Y. Seed-Specific Overexpression of Phytoene Synthase: Increase in Carotenoids and Other Metabolic Effects. *Plant J.* **1999**, *20*, 401−412.
(50) Llorente, B.; Torres-Montilla, S.; Morelli, L.; Florez-Sarasa, I.; Matus, J. T.; Ezquerro, M.; D'Andrea, L.; Houhou, F.; Majer, E.; Picó, B.; Cebolla, J.; Troncoso, A.; Fernie, A. R.; Daròs, J.-A.; Rodriguez-Concepcion, M. Synthetic Conversion of Leaf Chloroplasts into Carotenoid-Rich Plastids Reveals Mechanistic Basis of Natural Chromoplast Development. *Proc. Natl. Acad. Sci. U.S.A.* **2020**, *117*, 21796−21803.
(51) Couso, I.; Vila, M.; Rodriguez, H.; Vargas, M. A.; León, R. Overexpression of an Exogenous Phytoene Synthase Gene in the Unicellular Alga *Chlamydomonas reinhardtii* Leads to an Increase in the Content of Carotenoids. *Biotechnol. Prog.* **2011**, *27*, 54−60.
(52) Galarza, J. I.; Gimpel, J. A.; Rojas, V.; Arredondo-Vega, B. O.; Henríquez, V. Over-Accumulation of Astaxanthin in Haematococcus Pluvialis through Chloroplast Genetic Engineering. *Algal Res.* **2018**, *31*, 291−297.
(53) Kang, C.; Zhai, H.; Xue, L.; Zhao, N.; He, S.; Liu, Q. A Lycopene β-Cyclase Gene, IbLCYB2, Enhances Carotenoid Contents and Abiotic Stress Tolerance in Transgenic Sweetpotato. *Plant Sci.* **2018**, *272*, 243−254.
(54) Moreno, J. C.; Cerda, A.; Simpson, K.; Lopez-Diaz, I.; Carrera, E.; Handford, M.; Stange, C. Increased Nicotiana Tabacum Fitness through Positive Regulation of Carotenoid, Gibberellin and Chlorophyll Pathways Promoted by Daucus Carota Lycopene β-Cyclase (Dclcyb1) Expression. *J. Exp. Bot.* **2016**, *67*, 2325−2338.
(55) Kössler, S.; Armarego-Marriott, T.; Tarkowská, D.; Turečková, V.; Agrawal, S.; Mi, J.; de Souza, L. P.; Schöttler, M. A.; Schadach, A.; Fröhlich, A.; Bock, R.; Al-Babili, S.; Ruf, S.; Sampathkumar, A.; Moreno, J. C. Lycopene β-Cyclase Expression Influences Plant Physiology, Development, and Metabolism in Tobacco Plants. *J. Exp. Bot.* **2021**, *72*, 2544−2569.
(56) Jahns, P.; Holzwarth, A. R. The Role of the Xanthophyll Cycle and of Lutein in Photoprotection of Photosystem II. *Biochim. Biophys. Acta, Bioenerg.* **2012**, *1817*, 182−193.
(57) D'Ambrosio, C.; Stigliani, A. L.; Giorio, G. Overexpression of CrtR-B2 (Carotene Beta Hydroxylase 2) from S. Lycopersicum L. Differentially Affects Xanthophyll Synthesis and Accumulation in Transgenic Tomato Plants. *Transgenic Res.* **2011**, *20*, 47−60.
(58) Du, H.; Wang, N.; Cui, F.; Li, X.; Xiao, J.; Xiong, L. Characterization of the β-Carotene Hydroxylase Gene DSM2 Conferring Drought and Oxidative Stress Resistance by Increasing Xanthophylls and Abscisic Acid Synthesis in Rice. *Plant Physiol.* **2010**, *154*, 1304−1318.
(59) Davison, P. A.; Hunter, C. N.; Horton, P. Overexpression of β-Carotene Hydroxylase Enhances Stress Tolerance in Arabidopsis. *Nature* **2002**, *418*, 203−206.
(60) Lauersen, K. J.; Baier, T.; Wichmann, J.; Wördenweber, R.; Mussgnug, J. H.; Hübner, W.; Huser, T.; Kruse, O. Efficient Phototrophic Production of a High-Value Sesquiterpenoid from the Eukaryotic Microalga *Chlamydomonas reinhardtii*. *Metab. Eng.* **2016**, *38*, 331−343.
(61) Huang, K.; Su, Z.; He, M.; Wu, Y.; Wang, M. Simultaneous Accumulation of Astaxanthin and β-Carotene in *Chlamydomonas reinhardtii* by the Introduction of Foreign β-Carotene Hydroxylase Gene in Response to High Light Stress. *Biotechnol. Lett.* **2022**, *44*, 321−331.
(62) Tan, C.-P.; Zhao, F.-Q.; Su, Z.-L.; Liang, C.-W.; Qin, S. Expression of β-Carotene Hydroxylase Gene (CrtR-B) from the Green Alga Haematococcus Pluvialis in Chloroplasts of *Chlamydomonas reinhardtii*. *J. Appl. Phycol.* **2007**, *19*, 347−355.
(63) Del Campo, J. A.; García-González, M.; Guerrero, M. G. Outdoor Cultivation of Microalgae for Carotenoid Production: Current State and Perspectives. *Appl. Microbiol. Biotechnol.* **2007**, *74*, 1163−1174.
(64) Howitt, C. A.; Pogson, B. J.; Cuttriss, A. J.; Mimica, J. L. Carotenoids. *Adv. Photosynth. Respir.* **2007**, 315−334.
(65) Rathod, J. P.; Vira, C.; Lali, A. M.; Prakash, G. Metabolic Engineering of *Chlamydomonas reinhardtii* for Enhanced β-Carotene and Lutein Production. *Appl. Biochem. Biotechnol.* **2020**, *190*, 1457−1469.
(66) Steiger, S.; Schäfer, L.; Sandmann, G. High-Light-Dependent Upregulation of Carotenoids and Their Antioxidative Properties in the Cyanobacterium Synechocystis PCC 6803. *J. Photochem. Photobiol. B Biol.* **1999**, *52*, 14−18.
(67) Zheng, K.; Wang, C.; Xiao, M.; Chen, J.; Li, J.; Hu, Z. Expression of Bkt and Bch Genes from Haematococcus Pluvialis in Transgenic Chlamydomonas. *Sci. China Life Sci.* **2014**, *57*, 1028−1033.
(68) Armenta, R. E.; Guerrero-Legarreta, I. Stability Studies on Astaxanthin Extracted from Fermented Shrimp Byproducts. *J. Agric. Food Chem.* **2009**, *57*, 6095−6100.
(69) Fields, F. J.; Ostrand, J. T.; Mayfield, S. P. Fed-Batch Mixotrophic Cultivation of *Chlamydomonas reinhardtii* for High-Density Cultures. *Algal Res.* **2018**, *33*, 109−117.
(70) Xie, X.; Lu, X.; Wang, L.; He, L.; Wang, G. High Light Intensity Increases the Concentrations of β-Carotene and Zeaxanthin in Marine Red Macroalgae. *Algal Res.* **2020**, *47*, No. 101852.
(71) Fu, W.; Gudmundsson, Ó.; Paglia, G.; Herjólfsson, G.; Andrésson, Ó. S.; Palsson, BØ.; Brynjólfsson, S. Enhancement of Carotenoid Biosynthesis in the Green Microalga Dunaliella Salina with Light-Emitting Diodes and Adaptive Laboratory Evolution. *Appl. Microbiol. Biotechnol.* **2013**, *97*, 2395−2403.
(72) López, M.-M.; Sánchez, E. D. R.; López, J. L. C.; Fernández, F. G. A.; Sevilla, J. M. F.; Rivas, J.; Guerrero, M. G.; Grima, E. M. Comparative Analysis of the Outdoor Culture of Haematococcus Pluvialis in Tubular and Bubble Column Photobioreactors. *J. Biotechnol.* **2006**, *123*, 329−342.
(73) Park, J. C.; Choi, S. P.; Hong, M.-E.; Sim, S. J. Enhanced Astaxanthin Production from Microalga, Haematococcus Pluvialis by Two-Stage Perfusion Culture with Stepwise Light Irradiation. *Bioprocess Biosyst. Eng.* **2014**, *37*, 2039−2047.
(74) Diao, J.; Song, X.; Zhang, L.; Cui, J.; Chen, L.; Zhang, W. Tailoring Cyanobacteria as a New Platform for Highly Efficient Synthesis of Astaxanthin. *Metab. Eng.* **2020**, *61*, 275−287.
(75) Jin, J.; Wang, Y.; Yao, M.; Gu, X.; Li, B.; Liu, H.; Ding, M.; Xiao, W.; Yuan, Y. Astaxanthin Overproduction in Yeast by Strain Engineering and New Gene Target Uncovering. *Biotechnol. Biofuels* **2018**, *11*, No. 230.
(76) Lauersen, K. J.; Kruse, O.; Mussgnug, J. H. Targeted Expression of Nuclear Transgenes in *Chlamydomonas reinhardtii* with a Versatile,

https://doi.org/10.1021/acssynbio.2c00616
ACS Synth. Biol. 2023, 12, 820−831

Modular Vector Toolkit. *Appl. Microbiol. Biotechnol.* **2015**, *99*, 3491−3503.
(77) Gutiérrez, S.; Wellman, G. B.; Lauersen, K. J. Teaching an Old 'Doc' New Tricks for Algal Biotechnology: Strategic Filter Use Enables Multi-Scale Fluorescent Protein Signal Detection. *Front. Bioeng. Biotechnol.* **2022**, *10*, No. 1700.
(78) Fischer, N.; Rochaix, J. D. The Flanking Regions of PsaD Drive Efficient Gene Expression in the Nucleus of the Green Alga *Chlamydomonas reinhardtii*. *Mol. Genet. Genomics* **2001**, *265*, 888−894.
(79) Yang, X.; Peng, J.; Pan, J. Nourseothricin N-Acetyl Transferase (NAT), a New Selectable Marker for Nuclear Gene Expression in Chlamydomonas. *Plant Methods* **2019**, *15*, No. 140.
(80) Neupert, J.; Karcher, D.; Bock, R. Generation of *Chlamydomonas* Strains That Efficiently Express Nuclear Transgenes. *Plant J.* **2009**, *57*, 1140−1150.
(81) Gorman, D. S.; Levine, R. P. Cytochrome f and Plastocyanin: Their Sequence in the Photosynthetic Electron Transport Chain of *Chlamydomonas reinhardi*. *Proc. Natl. Acad. Sci. U.S.A.* **1965**, *54*, 1665−1669.
(82) Kropat, J.; Hong-Hermesdorf, A.; Casero, D.; Ent, P.; Castruita, M.; Pellegrini, M.; Merchant, S. S.; Malasarn, D. A Revised Mineral Nutrient Supplement Increases Biomass and Growth Rate in *Chlamydomonas reinhardtii*. *Plant J.* **2011**, *66*, 770−780.
(83) Kindle, K. L. High Frequency Nuclear Transformation of *Chlamydomonas reinhardtii*. *Proc. Natl. Acad. Sci. U.S.A.* **1990**, *87*, 1228−1232.
(84) López-paz, C.; Liu, D.; Geng, S.; Umen, J. G. Identification of *Chlamydomonas reinhardtii* Endogenous Genic Flanking Sequences for Improved Transgene Expression. *Plant J.* **2018**, *92*, 1232−1244.
(85) Sizova, I.; Fuhrmann, M.; Hegemann, P. A *Streptomyces rimosus* AphVIII Gene Coding for a New Type Phosphotransferase Provides Stable Antibiotic Resistance to *Chlamydomonas reinhardtii*. *Gene* **2001**, *277*, 221−229.

https://doi.org/10.1021/acssynbio.2c00616
ACS Synth. Biol. 2023, 12, 820−831